On the energy spectra of one-dimensional quasi-periodic systems

1988 J. Phys. C: Solid State Phys. 21 4311

(http://iopscience.iop.org/0022-3719/21/23/014)

J. Phys. C: Solid State Phys. **21** (1988) 4311–4324. Printed in the UK

On the energy spectra of one-dimensional quasi-periodic systems

Hong-ru Ma† and Chien-Hua Tsai‡

†Institute of Solid State Physics, Nanjing University, Nanjing, People's Republic of China

‡Centre of Theoretical Physics, CCAST (World Laboratory), Beijing, and Institute of Condensed Matter Physics, Jiao-Tong University, Shanghai, People's Republic of China

Received 2 November 1987, in final form 1 February 1988

Abstract. The Cantor set character of the electronic energy spectrum of a one-dimensional quasi-crystal in the form of a Fibonacci sequence is analysed under the tight-binding approximation by means of a renormalisation procedure. The electronic structure of quasi-periodic superlattices is also studied with the conclusion that there scarcely exists any notable difference from periodic superlattices.

Since the observation of fivefold symmetry by Schechtman *et al* (1984) in the x-ray diffraction pattern of $Al_{0.86}Mn_{0.14}$ quenched alloy, the discovery of quasi-crystals has stimulated wide interest and a range of research. Levine and Steinhardt (1984) suggested immediately after Schechtman *et al* (1984), a model of fivefold symmetry with long-range order. A number of authors (Bak 1985, Mermin 1985, Jaric 1985) discussed then the stability of icosahedral systems on the basis of the Landau theory. Very recently, Widom *et al* (1987) investigated a simple two-dimensional Lennard-Jones system with two components by Monte Carlo simulation. They obtained quasi-crystalline structure in equilibrium state with tenfold symmetry.

The electron and phonon structures of quasi-crystals have been investigated, too. Lu *et al* (1986) and Odagaki and Nguyen (1986) computed separately the lattice vibration spectra of one- and two-dimensional quasi-crystals. In a previous correspondence, the present authors (Ma *et al* 1986) reported results of computation of the electronic densities of states for a one-dimensional Fibonacci chain. Hu and Ting (1986) evaluated the electric resistivity of a one-dimensional quasi-crystal. Their conclusion is that there exist two categories of electronic states contributing very differently to the resistance, one corresponding to localised and the other corresponding to extended or tunnelling states.

The present paper is devoted firstly to an analysis of the Cantor set character of the electronic energy spectrum of a one-dimensional tight-binding quasi-crystal and secondly to an investigation of the electron structures of quasi-periodic superlattices. In our previous publication (Ma *et al* 1986), we have evaluated the electronic density of states (DOS) of a tight-binding model of a one-dimensional Fibonacci chain (see figure 1) described by the following Hamiltonian:

$$H = \sum_i |i\rangle \varepsilon_i \langle i| + \sum_{i,j} |i\rangle T_{ij} \langle j| \tag{1}$$

0022-3719/88/234311 + 14 $02.50

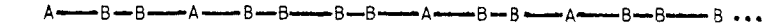

Figure 1. A schematic representation of a one-dimensional Fibonacci quasi-crystal. A and B signify possible different atomic levels.

where

$$\varepsilon_i = \begin{cases} \varepsilon_A & i \in A \\ \varepsilon_B & i \in B \end{cases} \tag{2}$$

and

$$T_{ij} = \begin{cases} T_L & j = i \pm 1, i \text{ and } j \text{ connected by a long bond} \\ T_S & j = i \pm 1, i \text{ and } j \text{ connected by a short bond} \\ 0 & \text{otherwise.} \end{cases} \tag{3}$$

Here we would like to supplement our previous results by showing in figures 2 and 3 the integrated DOS defined by

$$D(E) = \int^E \rho(E')\,\mathrm{d}E' \tag{4}$$

with $\rho(E)$ being the DOS obtained previously. It can be seen that the $D(E)$ curves display steps in one-to-one correspondence with occurrence of gaps in the $\rho(E)$ histograms (see figures 3 and 4 of Ma *et al* 1986). Two distinct steps can be seen when T_S is slightly larger than T_L. When the difference between T_S and T_L becomes larger, these main steps become wider and secondary steps appear. With still larger difference between T_S and T_L still smaller steps appear between the secondary steps. However, the height of both a main step or a smaller step remains constant independent of the value of $T_S - T_L$.

In figures 4 and 5 we display successive magnifications of $D(E)$ and $\rho(E)$ for a Fibonacci chain containing 25000 atoms. The self-similarity is evident in these figures showing the Cantor set structure of the electronic energy spectrum. In § 1 below we shall explain the above mentioned characteristics of the electronic energy spectrum and then in § 2 we shall consider the energy spectra of electrons in superlattices.

1. Renormalisation analysis of the electronic structure of one-dimensional quasi-crystals

Before analysing the electronic structure, we would like to remind readers of the self-similarity in the Fibonacci sequence:

S_1: L

S_2: LS

S_3: LSL

S_4: LSLLS

S_5: LSLLSLSL

S_6: LSLLSLSLLSLLS

. . . . . .

$S_n = S_{n-1}S_{n-2}$.

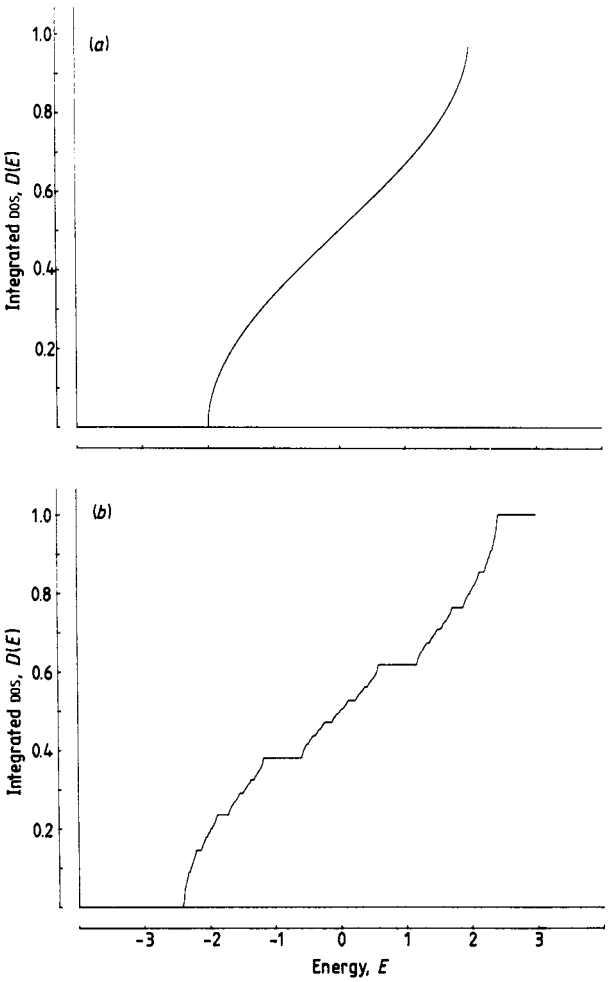

Figure 2. The integrated DOS of a one-dimensional Fibonacci chain of 10000 atoms in the symmetrical case: $\varepsilon_A = \varepsilon_B = 0$, $T_L = 1$, $T_S =$ (*a*) 1, (*b*) 1.5.

This means that starting with mth generation and identifying S_m, S_{m+1} with S, L respectively (e.g. setting $S_2 = LS = S'$ and $S_3 = LSL = L'$), we obtain once more the original sequence. We shall see this property has direct consequences on the electronic structure.

Now we turn to disclose the self-similarity structure in the electronic energy spectrum using renormalisation transformations (Niu and Mori 1986). Consider first, for simplicity, the case $\varepsilon_A = \varepsilon_B$. We begin with the case $T_L = 0$. The Fibonacci chain becomes, then, a one-dimensional array consisting of isolated atoms A and diatomic molecules composed of two B atoms. The energy eigenvalue of an electron on an isolated A atom is $E = 0$. On the other hand, a diatomic molecule has a bonding and an antibonding state, corresponding, respectively, to the energy eigenvalues $E = \mp T_S$. Thus the energy spectrum consists of three discrete levels: $E = 0, \pm T_S$. In the limit of an infinitely long Fibonacci chain, the number of long bonds to the number of short bonds is $N_L/N_S = \tau^{-1} = \frac{1}{2}(5^{1/2} + 1)$, where $\tau = \frac{1}{2}(5^{1/2} - 1)$ is the golden mean. Each short bond connects two B atoms and there is an A atom or a B molecule between any two

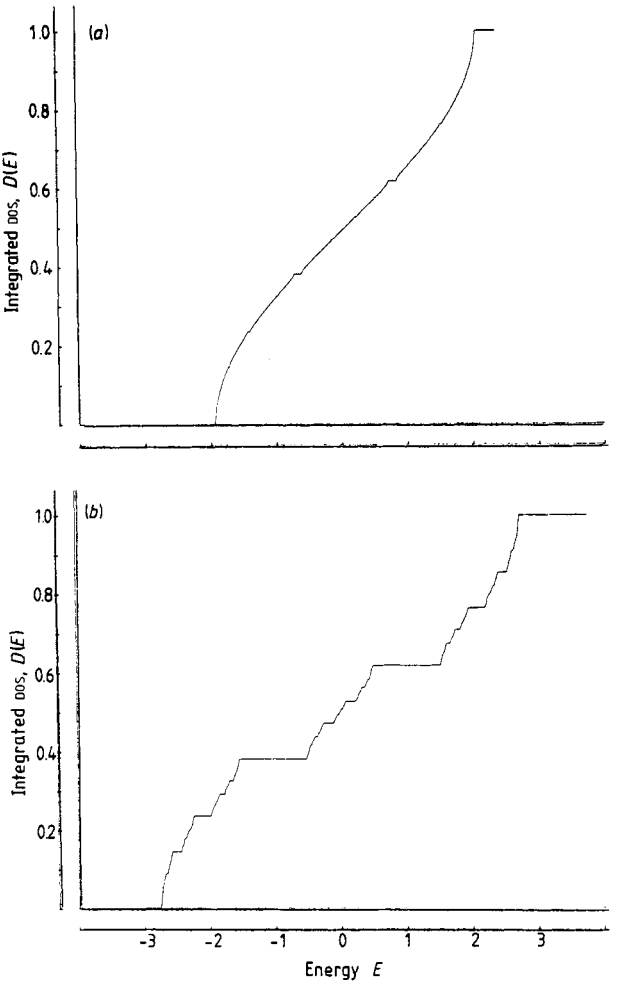

Figure 3. The integrated DOS of a one-dimensional Fibonacci chain of 10000 atoms in the asymmetrical case: $\varepsilon_A = 0$, $\varepsilon_B = 0.2$, $T_L = 1$, $T_S = (a)$ 1, (b) 1-9-

neighbouring long bonds. Let the numbers of A and B atoms be N_A and N_B, respectively, then by the above analysis, $N_B = 2N_S$ whereas $N_A = N_L - N_S$, so that $N_A/N_B = (2\tau)^{-1} - \frac{1}{2}$. Thus, the fractions of A and B atoms are, separately, τ^3 and $2\tau^2$. It follows that the DOS of the three levels are, respectively,

$$\rho(E = 0) = \tau^3$$
$$\rho(E = \pm T_S) = \tau^2. \tag{5}$$

The integrated DOS consists of three steps with respective heights: $\tau^2 = 0.38196601\ldots$, $\tau^2 + \tau^3 = 0.61803398\ldots$ and $2\tau^2 + \tau^3 = 1$, in agreement with results of numerical computation (see figures 2 and 3): 0.382, 0.618 and normalisation.

Consider next the case $T_L \neq 0$. For each degenerate level an equivalent Hamiltonian can be constructed in similarity to the original one, accomplishing thus a renormalisation transformation. Consider first the level $E = 0$ of an isolated atom. With a non-zero T_L,

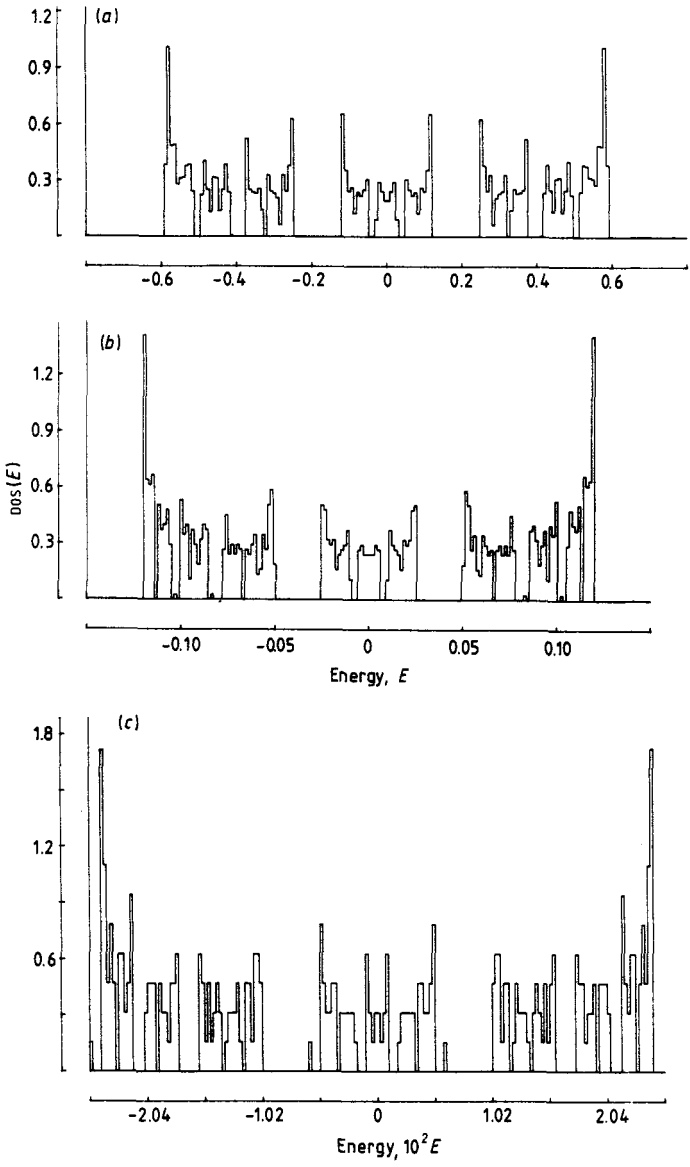

Figure 4. The electronic DOS of a one-dimensional Fibonacci chain of 25000 atoms in the symmetrical case with successive magnified views. $\varepsilon_A = \varepsilon_B = 0$, $T_L = 1$, $T_S = 1.5$.

each atom A is coupled to nearest atoms on both sides via molecules B. We proceed to calculate the effective coupling. Two cases must be distinguished: two nearest atoms are separated by one or two molecules. In the first case as shown in figure 6, we can write the following Schrödinger's equations:

$$\begin{aligned} T_L\psi_{n-1} + T_L\psi_{n+1} &= E\psi_n \\ T_L\psi_n + T_S\psi_{n+2} &= E\psi_{n+1} \\ T_S\psi_{n+1} + T_L\psi_{n+3} &= E\psi_{n+2}. \end{aligned} \tag{6}$$

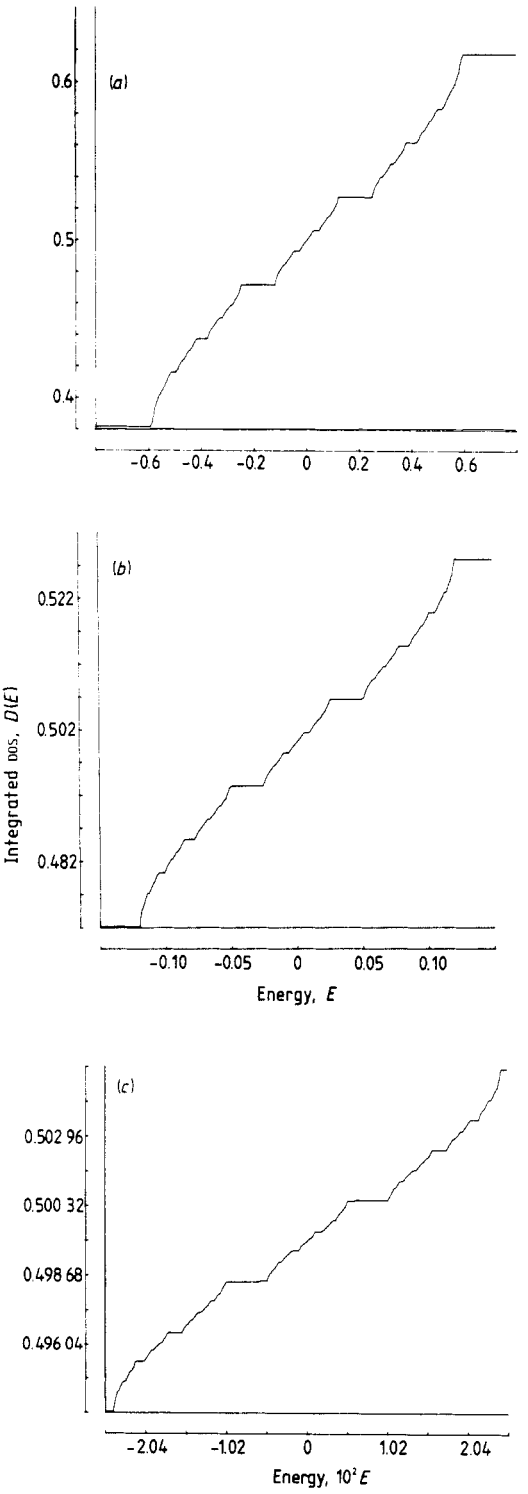

Figure 5. The integrated DOS of a one-dimensional Fibonacci chain of 25000 atoms in the symmetrical case with successive magnitifed views. $\varepsilon_A = \varepsilon_B = 0$, $T_L = 1$, $T_S = 1.5$.

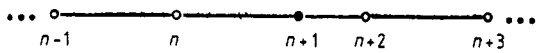

Figure 6. Two 'atoms' n and $n+3$ coupled via a 'molecule', $(n+1, n+2)$.

Solving for ψ_{n+1} from the third line of (6) and substituting into the first line, we have

$$T_L\psi_{n-1} - T_L^2 T_S^{-1}\psi_{n+3} = E\psi_n \tag{7}$$

by neglecting small terms in view of the fact that we are considering the level $E = 0$. Comparing with the first line of (6), we know the effective coupling strength is $T_S' = -T_L^2 T_S^{-1}$. For the case of two atoms separated by two molecules (figure 7), the Schrödinger's equations are:

$$\begin{aligned}
T_L\psi_{n-1} + T_L\psi_{n+1} &= E\psi_n \\
T_L\psi_n + T_S\psi_{n+2} &= E\psi_{n+1} \\
T_S\psi_{n+1} + T_L\psi_{n+3} &= E\psi_{n+2} \\
T_L\psi_{n+2} + T_S\psi_{n+4} &= E\psi_{n+3} \\
T_S\psi_{n+3} + T_L\psi_{n+5} &= E\psi_{n+4}.
\end{aligned} \tag{8}$$

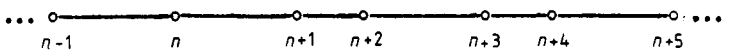

Figure 7. Two 'atoms' n and $n+5$ coupled via two 'molecules': $(n+1, n+2)$ and $(n+3)$, $n+4)$.

By the same procedure, we obtain

$$T_L\psi_{n-1} + T_L^3 T_S^{-1}\psi_{n+5} = E\psi_n. \tag{9}$$

Hence, the effective coupling strength is $T_L' = T_L^3 T_S^{-1}$. Replacing a bond between two A atoms via a single molecule with T_S' and a bond via two molecules with T_L', we obtain again a Fibonacci chain. Setting $T_L' = 0$ in the new Fibonacci crystal, we obtain the new 'atomic' and 'molecular' levels: $E = 0; \pm T_S'$. An identical analysis yields the same heights of the main steps in the integrated DOS as above. Since the DOS of the $E = 0$ level before the transformation is τ^3, the height of the first secondary step relative to the first main step is $\tau^2\tau^3 = \tau^5$, whereas that of the next secondary step is $\tau\,\tau^3 = \tau^4$, with corresponding absolute heights: $\tau^2 + \tau^5 = 0.47213595\ldots$ and $\tau^2 + \tau^4 = 0.52786404\ldots$. Results of numerical computation are 0.472 and 0.528 (figures 2 and 3).

In order to treat the molecular levels: $E = \pm T_S$, we note that a molecule may couple directly to another neighbouring molecule or indirectly via an atom. In the case of direct coupling (figure 8), we have

$$\begin{aligned}
T_L\psi_{n-1} + T_S\psi_{n+1} &= E\psi_n \\
T_S\psi_n + T_L\psi_{n+2} &= E\psi_{n+1} \\
T_L\psi_{n+1} + T_S\psi_{n+3} &= E\psi_{n+2} \\
T_S\psi_{n+2} + T_L\psi_{n+4} &= E\psi_{n+3}.
\end{aligned} \tag{10}$$

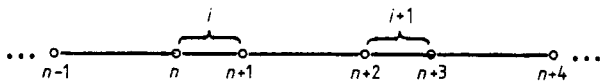

Figure 8. Two 'molecules', $i(n, n+1)$ and $i+1$ $(n+2, n+3)$, in direct coupling.

From figure 8, the bonding and anti-bonding states of the ith and the $(i+1)$th molecules, corresponding to the energy eigenvalues $E = \pm T_S$ are

$$\begin{aligned} \psi^i_{\pm} &= 2^{-1/2}(\psi_n \pm \psi_{n+1}) \\ \psi^{i+1}_{\pm} &= 2^{-1/2}(\psi_{n+2} \pm \psi_{n+3}). \end{aligned} \tag{11}$$

Substituting for ψ_n, ψ_{n+1}, ψ_{n+2} and ψ_{n+3} from (11) into (10), we have after simplifications

$$\begin{aligned} &2^{-1/2}T_L\psi_{n-1} + \tfrac{1}{2}T_L\psi^{i+1}_{+} - \tfrac{1}{2}T_L\psi^{i+1}_{-} = (E - T_S)\psi^i_{+} \\ &\tfrac{1}{2}T_L\psi^i_{+} - \tfrac{1}{2}T_L\psi^i_{-} + 2^{-1/2}T_L\psi_{n+4} = (E - T_S)\psi^{i+1}_{+} \\ &-2^{-1/2}T_L\psi_{n-1} + \tfrac{1}{2}T_L\psi^{i+1}_{+} - \tfrac{1}{2}T_L\psi^{i+1}_{-} = (E + T_S)\psi^i_{-} \\ &-\tfrac{1}{2}T_L\psi^i_{+} - \tfrac{1}{2}T_L\psi^i_{-} + 2^{-1/2}T_L\psi_{n+4} = (E + T_S)\psi^{i+1}_{-}. \end{aligned} \tag{12}$$

In the lowest order of approximation, when $E \simeq T_S$, the couplings between the bonding and anti-bonding states can be neglected. We omit thus all terms containing ψ^i_- and ψ^{i+1}_- (ψ^i_+ and ψ^{i+1}_+) in the equations for ψ^i_+ and ψ^{i+1}_+ (ψ^i_- and ψ^{i+1}_-) and conclude, thereby, that the effective coupling strength between anti-bonding (bonding) molecules is $\frac{1}{2}T_L$ ($-\frac{1}{2}T_L$).

The same analysis applied to molecules coupled indirectly via an atom yields an effective coupling strength between either anti-bonding or bond molecules as $\frac{1}{2}T_L^2T_S^{-1}$ (figure 9). Consider now a molecule as a single entity and describe, respectively, the

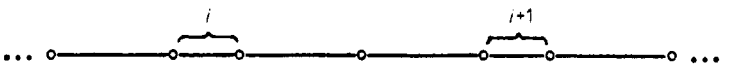

Figure 9. Two 'molecules', i and $i+1$, in indirect coupling via an 'atom'.

direct and indirect couplings with effective bonds by $T'_S = \pm\frac{1}{2}T_L$ and $T'_L = \frac{1}{2}T_L^2T_S^{-1}$; we again obtain a Fibonacci crystal. It follows that the anti-bonding level splits into three: $E = T_S$, and $T_S \pm T'_S = T_S \mp \frac{1}{2}T_L$. Since the DOS of the original level $E = T_S$ is τ^2, those of the three split levels are:

$$\rho(T_S - \tfrac{1}{2}T_L) = \tau^2\tau^2 = \tau^4 \qquad \rho(T_S) = \tau^2\tau^3 = \tau^5 \qquad \rho(T_S + \tfrac{1}{2}T_L) = \tau^2\tau^2 = \tau^4. \tag{13}$$

Two secondary steps appear in the integrated DOS with relative heights in respect of the second main step: τ^4 and τ^3 and absolute heights $\tau + \tau^4 = 0.7693202\ldots$, $\tau + \tau^3 = 0.85410196\ldots$, in contrast to the values 0.764 and 0.854 from numerical computation.

In a similar manner we obtain the absolute heights of the secondary steps arising from the bonding level as $\tau^4 = 0.14589803\ldots$ and $\tau^3 = 0.23606797\ldots$ in contrast to 0.146 and 0.236 by numerical evaluation.

The renormalisation process can be carried on indefinitely. We list in the following table 1 the absolute heights of the steps of the first three orders. Successive renormalisation transformations generate, therefore, sub-bands and gaps of higher and higher orders in the energy spectrum and steps of successive orders in the integrated DOS, resulting in a Cantor set structure.

Table 1. The absolute heights of steps in the integrated DOS. $\tau = \frac{1}{2}(5^{1/2} - 1) = 0.61803399\ldots$.

Order of steps in $D(E)$		
1	2	3
		τ^6
		τ^5
	τ^4	
		$\tau^7 + \tau^4$
		$\tau^6 + \tau^4$
	τ^3	
		$\tau^6 + \tau^3$
		$\tau^5 + \tau^3$
τ^2		
		$\tau^6 + \tau^2$
		$\tau^5 + \tau^2$
	$\tau^5 + \tau^2$	
		$\tau^7 + \tau^5 + \tau^2$
		$\tau^6 + \tau^5 + \tau^2$
	$\tau^4 + \tau^2$	
		$\tau^6 + \tau^4 + \tau^2$
		$\tau^5 + \tau^4 + \tau^2$
τ		
		$\tau^6 + \tau$
		$\tau^5 + \tau$
	$\tau^4 + \tau$	
		$\tau^7 + \tau^4 + \tau$
		$\tau^6 + \tau^4 + \tau$
	$\tau^3 + \tau$	
		$\tau^6 + \tau^3 + \tau$
		$\tau^5 + \tau^3 + \tau$
1		

It should be pointed out that the preceding analysis is based upon the conditions $|T_L/T_S| \ll 1$ and $\varepsilon_A = \varepsilon_B = 0$. However, numerical computation implies that results of the above analysis are correct even though $T_L \leqslant T_S$. When $\varepsilon_B \neq 0$, there are two cases. In the first case when ε_B is small relative to T_S, a non-vanishing ε_B does not affect the above conclusions. In the second case when ε_B is large, so that the order of arrangement of 'atomic' and 'molecular' levels is modified, the heights of the steps will be affected. Nevertheless, the ideas of the analysis still works. Discussions in this case will be postponed for a later publication.

2. Electronic structure of quasi-periodic superlattices

It is of interest to ask whether the above-explained structure in the energy spectrum can be detected in a more realistic physical system, such as quasi-periodic superlattices (Hu *et al* 1986; Merlin *et al* 1985). We shall show in this section that, unfortunately, the answer is in the negative.

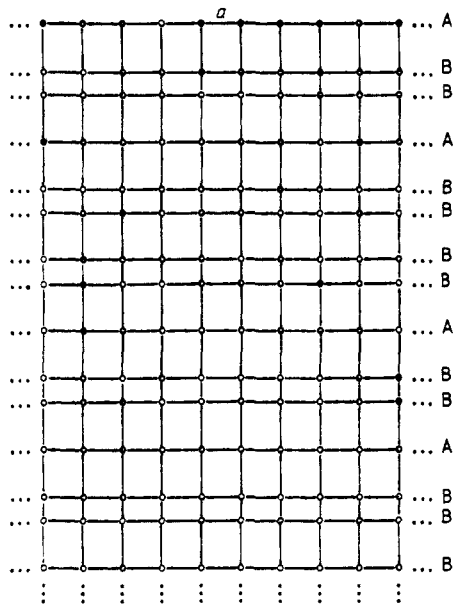

Figure 10. Schematic representation of a Fibonacci quasi-superlattice, where a is the lattice spacing of the periodic chains (planes).

Suppose an infinite number of one-dimensional periodic chains or two-dimensional square lattices are arranged in a Fibonacci sequence as shown in figure 10. We prescribe a periodic atomic chain (plane) connecting to nearest-neighbouring chains (planes) on both sides by long bonds as an A atomic chain (plane) and all other chains (planes) as B atomic chains (planes). The tight-binding Hamiltonian of the system can be written

$$H = \sum_i |i\rangle \varepsilon_i \langle i| + \sum_{i,j} |i\rangle T_{ij} \langle j|$$

where

$$\varepsilon_i = \begin{cases} \varepsilon_A & i \in A \\ \varepsilon_B & i \in B \end{cases} \tag{14}$$

and

$$T_{ij} = \begin{cases} T_L & (i,j) = (n,n),\ i \text{ and } j \text{ connected by a long bond} \\ T_S & (i,j) = (n,n),\ i \text{ and } j \text{ connected by a short bond} \\ T_A & (i,j) = (n,n),\ i \text{ and } j \text{ connected by a periodic A bond} \\ T_B & (i,j) = (n,n),\ i \text{ and } j \text{ connected by a periodic B bond} \\ 0 & \text{otherwise.} \end{cases} \tag{15}$$

Transforming to the Fourier representation in the directions of periodic arrangement,

$$H = \sum_{k,n} |k,n\rangle \varepsilon_n(k) \langle k,n| + \sum_{k,n} \{T_{n,n-1} |k,n\rangle \langle k,n-1| + T_{n,n+1} |k,n\rangle \langle k,n+1| + \text{CC}\} \tag{16}$$

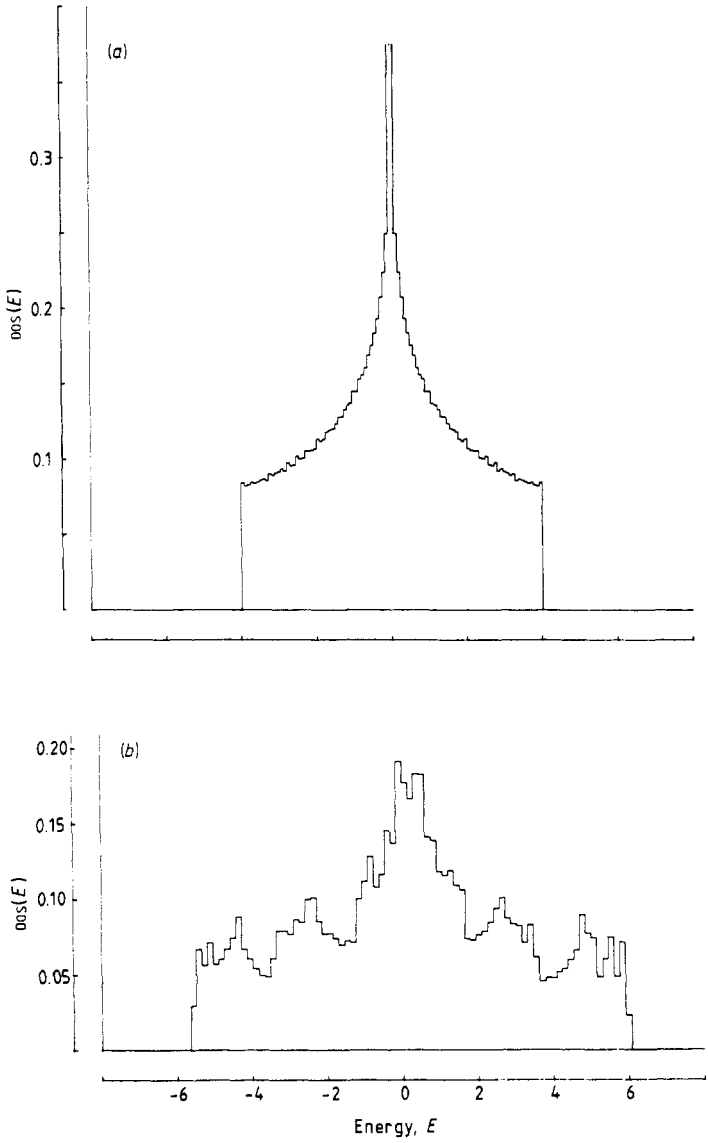

Figure 11. The electronic DOS of a two-dimensional Fibonacci quasi-superlattice. (*a*) $\varepsilon_A = \varepsilon_B = 0$, $T_1 = T_2 = 1$, $T_L = T_S = 1$; (*b*) $\varepsilon_A = 0$, $\varepsilon_B = 0.5$, $T_1 = T_2 = 1.5$, $T_L = 1$, $T_S = 1.9$.

where k is a Bloch vector. Writing $H = \Sigma_k H_k$, then H_k is the Hamiltonian of a one-dimensional quasi-crystal. In (15),

$$\varepsilon_n(k) = \begin{cases} \varepsilon_A + 2T_A \cos(ka) & \text{when } n \text{ is an A chain} \\ \varepsilon_B + 2T_B \cos(ka) & \text{when } n \text{ is a B chain} \end{cases} \tag{17}$$

in the case of a two-dimensional quasi-periodic superlattice and

$$\varepsilon_n(k) = \begin{cases} \varepsilon_A + 2T_A[\cos(k_x a) + \cos(k_y a)] & \text{when } n \text{ is an A plane} \\ \varepsilon_B + 2T_B[\cos(k_x a) + \cos(k_y a)] & \text{when } n \text{ is a B plane} \end{cases} \tag{18}$$

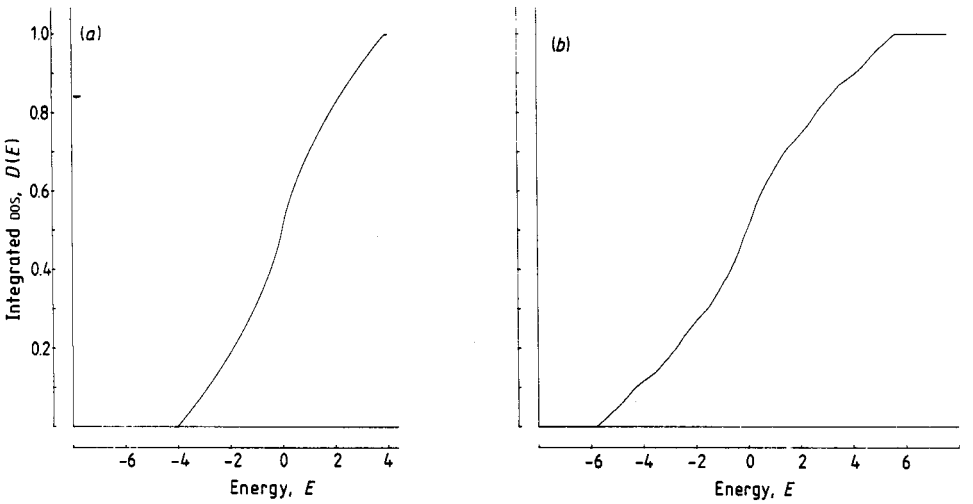

Figure 12. The integrated DOS of a two-dimensional Fibonacci quasi-superlattice with identical parameters as in figure 11.

in the case of a three-dimensional quasi-periodic superlattice, whereas

$$T_{n,n\pm1} = \begin{cases} T_L & n \text{ and } n \pm 1 \text{ connected by a long bond} \\ T_S & n \text{ and } n \pm 1 \text{ connected by a short bond.} \end{cases} \tag{19}$$

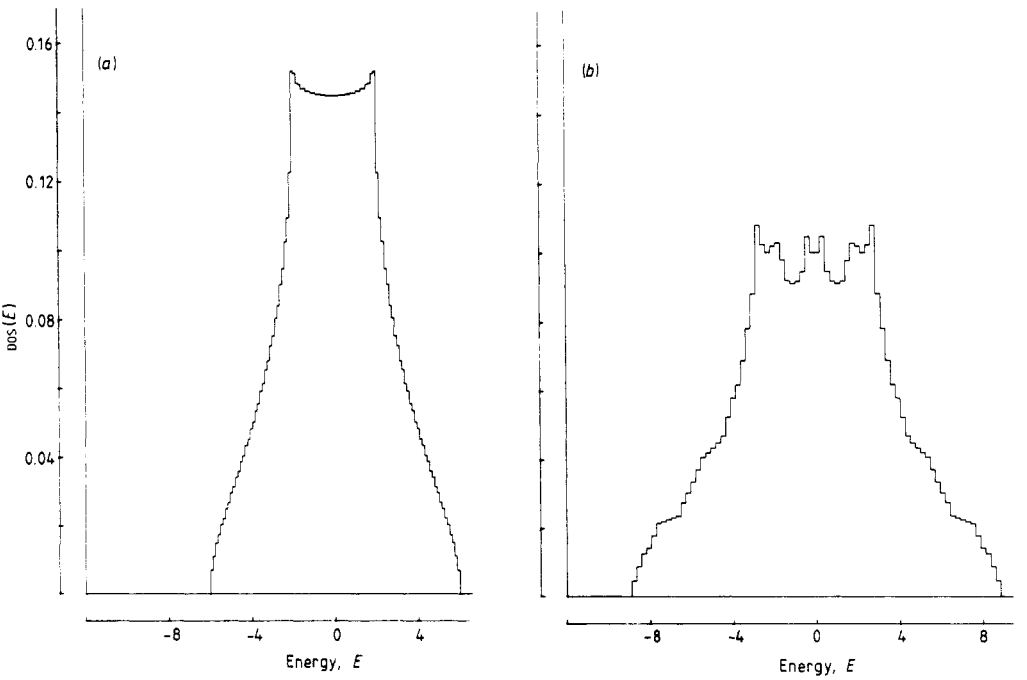

Figure 13. The electronic DOS of a three-dimensional Fibonacci quasi-superlatice. (*a*) $\varepsilon_A = \varepsilon_B = 0$, $T_1 = T_2 = T_L = T_S = 1$; (*b*) $\varepsilon_A = \varepsilon_B = 0$, $T_1 = T_2 = 1.5$, $T_L = 1$, $T_S = 1.9$.

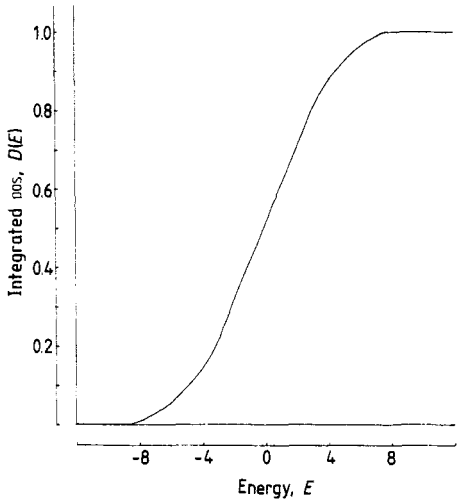

Figure 14. The integrated DOS of a three-dimensional Fibonacci quasi-superlattice. $\varepsilon_A = \varepsilon_B = 0$, $T_1 = T_2 = 1.5$, $T_L = 1$, $T_S = 1.9$.

For a fixed k, H_k is a tridiagonal matrix. The corresponding DOS $\rho(k, E)$ can be computed by means of the method of negative eigenvalues (Dean 1972, Ma *et al* 1986). The total DOSs are then given by

$$\rho(E) = (2\pi)^{1-D} \int \mathrm{d}^{D-1}k(k, E) \qquad D(E) = (2\pi)^{1-D} \int^{E} \mathrm{d}E' \int \mathrm{d}^{D-1}k(k, E') \quad (20)$$

D being the dimensionality of the superlattice.

The results of computation are given in figures 11 to 14. In the case of two-dimensional superlattices, only very indistinct, blurred 'steps' can be seen in the integrated DOS curves, while in the case of three-dimensional superlattices, the DOS histograms and the integrated DOS curves are essentially the same as in the case of an ordinary three-dimensional crystal with periodic lattice structure, no important characteristics arising from the quasi-periodicity are detectable. We conclude, therefore, there exist no important differences in the bulk properties, such as the specific heat, between quasi-periodic and periodic superlattices. Nevertheless, the Cantor set structure is still observable, in the case of a quasi-superlattice, by investigating any physical process for which only the energy spectrum at a definite point in the (one- or) two-dimensional Brillouin zone is concerned (Ma and Tsai 1987, Todd *et al* 1986).

Acknowledgment

The authors would like to acknowledge helpful discussions by Dr G D Pang.

References

Bak P 1985 *Phys. Rev. Lett.* **54** 1517
Dean P 1972 *Rev. Mod. Phys.* **44** 127
Hu A, Tien C, Li X J, Wang Y H and Feng D 1986 *Phys. Lett.* **119A** 313

Hu P and Ting C S 1986 *Phys. Rev.* B **34** 8331
Jaric M V 1985 *Phys. Rev. Lett.* **55** 607
Levine D and Steinhardt P J 1984 *Phys. Rev. Lett.* **53** 2477
Lu J P, Odagaki T and Birman J L 1986 *Phys. Rev.* B **33** 4809
Ma H R, Xu T and Tsai C H 1986 *J. Phys. C: Solid State Phys.* **19** L823
Ma H R and Tsai C H 1987 *Phys. Rev.* B **35** 9295
Merlin R, Bajema K, Clarke R, Juang Y and Bhattachanya A 1985 *Phys. Rev. Lett.* **55** 1768
Mermin N D and Troian S M 1985 *Phys. Rev. Lett.* **54** 1524
Niu P and Nori F 1986 *Phys. Rev. Lett.* **57** 2057
Odagaki T and Nguyen D 1986 *Phys. Rev.* B **33** 2184
Schechtman D, Blech I, Gratias D and Cahn J W 1984 *Phys. Rev. Lett.* **53** 1951
Todd J, Merlin R, Clarke R, Mohanty K M and Axe J D 1986 *Phys. Rev. Lett.* **57** 1157
Widom M, Stradburg K J and Swendsen R H 1987 *Phys. Rev. Lett.* **58** 706